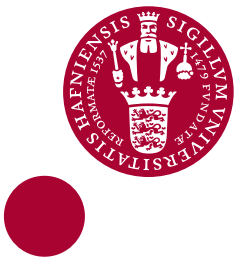

Ice core evidence for a 20th century increase in surface mass balance in coastal Dronning Maud Land, East Antarctica

Philippe, Morgane; Tison, Jean-Louis; Fjosne, Karen; Hubbard, Bryn; Kjær, Helle Astrid; Lenaerts, Jan T. M.; Drews, Reinhard; Sheldon, Simon Geoffrey; De Bondt, Kevin; Claeys, Philippe; Pattyn, Frank

Published in:
Cryosphere

DOI:
10.5194/tc-10-2501-2016

Publication date:
2016

Document version
Publisher's PDF, also known as Version of record

The Cryosphere, 10, 2501–2516, 2016
www.the-cryosphere.net/10/2501/2016/
doi:10.5194/tc-10-2501-2016

The Cryosphere Open Access EGU

Ice core evidence for a 20th century increase in surface mass balance in coastal Dronning Maud Land, East Antarctica

Morgane Philippe[1], Jean-Louis Tison[1], Karen Fjøsne[1], Bryn Hubbard[2], Helle A. Kjær[3], Jan T. M. Lenaerts[4], Reinhard Drews[5], Simon G. Sheldon[3], Kevin De Bondt[6], Philippe Claeys[6], and Frank Pattyn[1]

[1]Laboratoire de Glaciologie, Département des Géosciences, Environnement et Société, Université Libre de Bruxelles, 1050 Brussels, Belgium
[2]Centre for Glaciology, Department of Geography and Earth Sciences, Aberystwyth University, Aberystwyth, SY23 3DB, UK
[3]Centre for Ice and Climate, Niels Bohr Institute, University of Copenhagen, Juliane Maries Vej 30, 2100, Copenhagen, Denmark
[4]Institute for Marine and Atmospheric Research Utrecht, Utrecht University, Princetonplein 5, 3584 CC Utrecht, the Netherlands
[5]Bavarian Academy for Sciences and Humanities, Alfons-Goppel-Strasse 11, 80539 Munich, Germany
[6]Department of Analytical Environmental and Geo-Chemistry, Vrije Universiteit Brussel, Pleinlaan 2, 1050 Brussels, Belgium

Correspondence to: Morgane Philippe (mophilip@ulb.ac.be)

Received: 1 February 2016 – Published in The Cryosphere Discuss.: 29 February 2016
Revised: 23 September 2016 – Accepted: 3 October 2016 – Published: 25 October 2016

Abstract. Ice cores provide temporal records of surface mass balance (SMB). Coastal areas of Antarctica have relatively high and variable SMB, but are under-represented in records spanning more than 100 years. Here we present SMB reconstruction from a 120 m-long ice core drilled in 2012 on the Derwael Ice Rise, coastal Dronning Maud Land, East Antarctica. Water stable isotope (δ^{18}O and δD) stratigraphy is supplemented by discontinuous major ion profiles and continuous electrical conductivity measurements. The base of the ice core is dated to AD 1759 ± 16, providing a climate proxy for the past $\sim$250 years. The core's annual layer thickness history is combined with its gravimetric density profile to reconstruct the site's SMB history, corrected for the influence of ice deformation. The mean SMB for the core's entire history is 0.47 ± 0.02 m water equivalent (w.e.) a^{-1}. The time series of reconstructed annual SMB shows high variability, but a general increase beginning in the 20th century. This increase is particularly marked during the last 50 years (1962–2011), which yields mean SMB of 0.61 ± 0.01 m w.e. a^{-1}. This trend is compared with other reported SMB data in Antarctica, generally showing a high spatial variability. Output of the fully coupled Community Earth System Model (CESM) suggests that, although atmospheric circulation is the main factor influencing SMB, variability in sea surface temperatures and sea ice cover in the precipitation source region also explain part of the variability in SMB. Local snow redistribution can also influence interannual variability but is unlikely to influence long-term trends significantly. This is the first record from a coastal ice core in East Antarctica to show an increase in SMB beginning in the early 20th century and particularly marked during the last 50 years.

1 Introduction

In a changing climate, it is important to know the surface mass balance (SMB, i.e. precipitation minus evaporation, sublimation, meltwater runoff, and/or erosion) of Earth's ice sheets as it is an essential component of their total mass balance, which directly affects sea level (Rignot et al., 2011). The average rate of Antarctic contribution to sea level rise is estimated to have increased from 0.08 [−0.10 to 0.27] mm a^{-1} for 1992–2001 to 0.40 [0.20 to 0.61] mm a^{-1} for 2002–2011, mainly due to increasing ice discharge from West Antarctica (Vaughan et al., 2013), where the present-day warming seems to be focused (Turner et al., 2005;

Bromwich et al., 2014; Ludescher et al., 2015). Some studies suggested that this increase in dynamic ice loss could be partly compensated for by a warming-related increase in precipitation (e.g. Krinner et al., 2007; Palerme et al., 2016) by the end of the 21st century, but this is subject to debate. For example, Frieler et al. (2015) argued on the basis of ice core data and modelling that past Antarctic SMB was positively correlated with air temperature during glacial–interglacial changes. However, Fudge et al. (2016) found that SMB and temperature have not always been positively correlated in West Antarctica.

A clear spatio-temporal pattern in Antarctic SMB change is yet to emerge. Figure 1 and Table S1 in the Supplement summarize results of SMB trends from studies based on ice cores, stake networks, and radar. For the continent as a whole, there appears to have been no significant long-term trend in SMB over the past few decades (Nishio et al., 2002; van de Berg et al., 2006; Monaghan et al., 2006; van den Broeke et al., 2006; Bromwich et al., 2011; Lenaerts et al., 2012; Wang et al., 2016). Accordingly, 69 % of studies show <10 % change over the last ~ 50 years relative to the last ~ 200 years. For example, Isaksson et al. (1996) found <3 % change at the EPICA drilling site (Amundsenisen) in Dronning Maud Land (DML) between 1865–1965 and 1966–1991. Considering studies comparing only the last 20 years with the last 200 years, the percentage reporting no significant trend falls from 69 to 46 %. The trends revealed over this time period are both negative and positive, although slightly in favour of the latter, with 18 % of studies showing a decrease of >10 and 36 % showing an increase of >10 %. These data compare with 9 and 21 % respectively of studies reporting SMB change over the past ~ 50 years. This analysis therefore hints at a recent increase in SMB change, whether positive or negative. Indeed, at some locations SMB change appears only to have begun ~ 20 years ago (e.g. Site M: Karlöf et al., 2005).

Regionally, East Antarctica appears to have experienced recent positive mass balance as a whole (Shepherd et al., 2012) and particularly at inland sites, e.g. at South Pole Station (Mosley-Thompson et al., 1999), Dome C (Frezzotti et al., 2005), Dome A (Ren et al., 2010; Ding et al., 2011), and DML (Moore et al., 1991; Oerter et al., 2000). However, in DML the picture is by no means clear, with some studies reporting little or no recent SMB change (Isaksson et al., 1999; Oerter et al., 1999, 2000; Hofstede et al., 2004; Fernandoy et al., 2010) and others reporting negative change, both inland (e.g. Anschütz et al., 2011) and near the coast (Kaczmarska et al., 2004: S100; Isaksson and Melvold, 2002: Site H; Isaksson et al., 1999: S20; Isaksson et al., 1996: Site E; Isaksson et al., 1999: Site M). Altnau et al. (2015) compiled DML SMB records and reported a statistically significant positive trend for the region's interior and a negative trend for the coast. In contrast, satellite data and regional climate models indicate a recent increase in precipitation in coastal East Antarctica (Davis et al., 2005; Lenaerts et al., 2012).

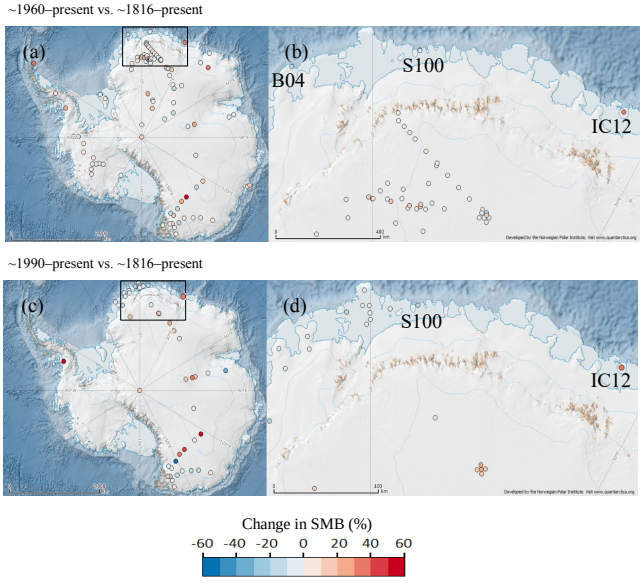

Figure 1. Location of IC12 and other ice cores referred to herein. **(a–b)** Difference in mean annual SMB between the period ~ 1960–present and the period ~ 1816–present (see Table S1 for exact periods and references); **(c–d)** same as **(a–b)** for the period ~ 1990–present compared with ~ 1816–present. Panels **(b)** and **(d)** are expansions of the framed areas in panels **(a)** and **(c)**.

Similarly, King et al. (2012) estimated on the basis of glacial isostatic adjustment modelling that a 60 ± 13 Gt a^{-1} mass increase calculated for the East Antarctic Ice Sheet during the last 20 years was concentrated along its coastal regions, particularly in DML. Indeed, coastal DML appears to have experienced several high SMB years since 2009 (Boening et al., 2012; Lenaerts et al., 2013), similar to positive trends in coastal West Antarctica (Thomas et al., 2008; Aristarain et al., 2004). Such increases are supported by calibrated regional atmospheric climate models, which indicate higher SMB along coastal sectors during the period 1980–2004 (e.g. van de Berg et al., 2006). Furthermore, Wang et al. (2016) reported that climate models generally underestimate SMB in coastal DML. This is broadly consistent with the analysis of Frezzotti et al. (2013), who compared sites with low SMB (<0.3 m water equivalent (w.e.) a^{-1}) with sites with high SMB (>0.3 m w.e. a^{-1}), reporting that most of the high SMB sites show an increase in SMB.

It is therefore apparent that, while there is a clear need for data from all of the coastal areas of East Antarctica (ISMASS Committee, 2004; van de Berg et al., 2006; Magand et al., 2007; Wang et al., 2016), there is particular uncertainty concerning the SMB history of the coastal region of DML. Indeed, although 17 of the records summarized in Table S1 report data from ice cores drilled below 1500 m above sea level and within 100 km of the DML coast, only two of these cover a period longer than 100 years: S100 (Kaczmarska et al., 2004) and B04 (Schlosser and Oerter, 2002), both in-

dicating a small negative trend (Fig. 1, Table S1). Despite this scarcity, SMB records from such cores are valuable for several reasons, including evaluating regional climate models (e.g. Lenaerts et al., 2014), calibrating internal reflection horizons in radio-echo sounding records (e.g. Fujita et al., 2011; Kingslake et al., 2014), and validating ice sheet flow and dating models (e.g. Parennin et al., 2007). Cores from coastal regions also generally provide higher temporal resolution than from the interior because SMB generally decreases with both elevation and distance from the coast (Frezzotti et al., 2005). Near the coast, ice rises represent ideal locations for palaeoclimate studies (Matsuoka et al., 2015) because they are undisturbed by upstream topography, lateral flow is almost negligible, and melt events are likely to be much less frequent than on ice shelves (Hubbard et al., 2013).

In this paper we report water stable isotope (δ^{18}O and δD), major ion data, and continuous electrical conductivity measurement (ECM) data along a 120 m-long ice core drilled on the Derwael Ice Rise (DIR) in coastal DML. We date the core base to AD 1759 ± 16 by layer counting. After correcting for dynamic vertical thinning, we calculate average SMB and annual SMB for the last ~ 250 years, i.e. across the Anthropocene transition, and compare them with other reported trends from the region.

2 Field site and methods

2.1 Field site

The study site is located in coastal DML, East Antarctica. A 120 m-long ice core, named IC12 after the project name IceCon, was drilled in 2012 on the crest of the DIR, which is 550 m thick (70°14′44.88″ S, 26°20′5.64″ E,; 450 m a.s.l.; Fig. 1).

Ice rises provide scientifically valuable drill sites because they are located close to the ocean (and hence sample coastal precipitation regimes) and because ground-penetrating radar data can easily identify drill sites on a local dome that are relatively undisturbed by horizontal flow. However, a number of regional factors complicate the interpretation of ice-core records on ice rises; for example, ice rises form topographic barriers with the capacity to disrupt atmospheric circulation on otherwise flat ice shelves. Orographic precipitation can thereby result in significantly high SMB values on the upwind sides of such ice rises, with corresponding precipitation shadows on the downwind side (Lenaerts et al., 2014). For the DIR in particular, the SMB on the upwind side is up to 2.5 times higher than on the downwind side (Callens et al., 2016). On top of this larger scale (~ 10 km) asymmetry, Drews et al. (2015) identified a small-scale (km) SMB oscillation near the crest, tentatively attributed to erosion at the crest, and subsequent redeposition on its downwind side. Radar stratigraphy shows that the local SMB maximum is located ~ 4 km upwind of the drill site (Figs. 1 and 4 in Drews et al., 2015). This means that the ice-core-derived SMB may sample a regime that varies at short spatial scales. Moreover, Drews et al. (2015) identified isochrone arches (a.k.a. Raymond bumps) beneath the DIR divide. This characteristic flow pattern causes ice at shallow to intermediate depths beneath the divide to be older than at comparable depths in the ice-rise flanks, necessitating a specific strain correction for the ice-core analysis, which we discuss below. However, both Drews et al. (2015) and Callens et al. (2016) suggested that the DIR has maintained its local crest for the last few thousand of years and possibly longer. By matching the radar stratigraphy to an ice-flow model, Drews et al. (2015) suggested that the DIR crest elevation is close to steady state and has potentially undergone modest surface lowering in the past. Both studies used a temporally constant SMB. Here we focus on the temporal variability and argue that, because the DIR has been stable in the past, we can draw conclusions with respect to the larger-scale atmospheric circulation patterns.

2.2 Ice coring and density analyses

The IC12 ice core was drilled with an Eclipse electromechanical ice corer in a dry borehole. The mean length of the core sections recovered after each run was 0.77 m and the standard deviation 0.40 m. The ice core is complete, except for the 100–101 m section, which fell back in the borehole and was recovered in broken pieces. Immediately after drilling, temperature (Testo 720 probe, inserted in a 4 mm diameter hole drilled to the centre of the core, precision ± 0.1 °C) and length were measured on each core section, which was then wrapped in a PVC bag, stored directly in a refrigerated container at -25 °C, and kept at this temperature until analysis at the home laboratory. Here, core sections were bisected lengthwise in a cold room at -20 °C. One half of the core section was used for ECM measurements and then kept as an archive, and the other half was sectioned for water stable isotope sampling and major ion analysis. Only a few very thin (1 mm) ice layers are present in the core. An optical televiewer-based best fit to discrete gravimetric density measurements, previously published (Hubbard et al., 2013), is used here to convert measured annual layer thicknesses to m w.e. (Sect. 2.3).

2.3 Annual layer counting and dating

2.3.1 Water stable isotopes and major ions

Using a clean bandsaw, half of each core section was resampled as a central bar of 30 mm × 30 mm square section. The outer part of the half-core was melted and stored in 4 mL bottles for subsequent δ^{18}O and δD analysis, completely filled to prevent contact with air. For major ion measurements, the inner bar was placed in a Teflon holder and further decon-

taminated by removing ∼ 2 mm from each face under a class-100 laminar flow hood using a methanol-cleaned microtome blade. Each 5 cm-long decontaminated section was then covered with a clean PE storage bottle, and the sample was cut loose from the bar by striking it perpendicular to the bar axis. Blank ice samples prepared from Milli-Q water were processed before every new core section and analysed for contamination.

Dating was achieved by annual layer counting identified from the stratigraphy of the δ^{18}O and δD isotopic composition of H_2O measured with a PICARRO L 2130-i cavity ring-down spectrometer (CRDS) ($\sigma = 0.05$ ‰ for δ^{18}O and 0.3 ‰ for δD). This composition was generally measured at 10 cm resolution in the top 80 m and 5 cm resolution below (See Supplement Fig. S1 for exact resolution). For sections of unclear isotopic seasonality, major ion analysis (Na^+, Cl^-, $SO_4^=$, NO_3^- and methylsuflonic acid (MSA)) was additionally carried out using a Dionex-ICS5000 liquid chromatograph, at 5 cm resolution. The system has a standard deviation of 2 ppb for Na^+ and $SO_4^=$, 8 ppb for Cl^-, 7 ppb for NO_3^-, and 1 ppb for MSA. Non-sea-salt sulfate was calculated as $nssSO_4 = [SO_4^=]_{tot} - 0.052 \times [Cl^-]$ following Mulvaney et al. (1992) and represents all $SO_4^=$ not of a marine aerosol origin. The ratio $Na^+ / SO_4^=$ was also calculated as an indicator of seasonal $SO_4^=$ production.

2.3.2 ECM measurements

ECM measurements were carried out in a cold room at −18 °C at the Centre for Ice and Climate, Niels Bohr Institute, University of Copenhagen, with a modified version of the Copenhagen ECM described by Hammer (1980). Direct current (1250 V) was applied at the surface of the freshly cut ice and electrical conductivity was measured at 1 mm resolution. The DC electrical conductivity of the ice, once corrected for temperature, depends principally on its acidity (Hammer, 1980; Hammer et al., 1994). This content varies seasonally and usually shows longer term localized maxima associated with sulfate production from volcanic eruptions. ECM can therefore be used both as a relative and an absolute dating tool.

As measurements were principally made in firn, we applied the technique described by Kjær et al. (2016) to correct for the effect of firn porosity on the amplitude of the signal. Because ECM scales inversely with air content, we multiplied the measured ECM signal by the ratio of the ice density to firn density (ρ_{ice}/ρ_{firn}), using the gravimetric density best fit from Hubbard et al. (2013). While there are millimetric-scale differences between the optical televiewer log and the ice core depth scales used to derive this best fit, the correlation provides an acceptably high coefficient of determination ($R^2 = 0.96$) for this purpose. ECM data were then smoothed with a 301-point first-order Savitsky–Golay filter (Savitsky and Golay, 1964) which eliminates peaks due to random noise and small-scale variations in material chemical composition, while preserving the larger peaks, including those due to volcanic eruptions. Finally, the ECM data were normalized by subtracting the mean and dividing by the standard deviation following Karlöf et al. (2000).

2.4 Corrections for ice flow

The compression of snow under its own weight involves not only vertical density changes, but also lateral deformation of the underlying ice. Failure to take the latter process into account would result in an underestimation of reconstructed initial annual layer thickness, and therefore of the SMB, especially within the deepest and hence oldest part of the record. We explore two different models to represent vertical strain rate evolution with depth: (i) strain rates derived from a full Stokes model that represent the full Raymond effect measured at the ice divide (Drews et al., 2015), and (ii) a modified Dansgaard–Johnsen model (Dansgaard and Johnsen, 1969) based on the description given in Cuffey and Paterson (2010).

The Drews et al. (2015) strain rate profile accounts for the best fit to radar layers at depth, taking into account a small amount of surface lowering ($0.03\,m\,a^{-1}$) and rheological anisotropy of the ice (run $A(n = 3)$, $dH = 100$, $\chi = 0.03\,m\,a^{-1}$, layer-depth SMB). The magnitude of applied surface lowering is small and does not alter the strain rates significantly compared to a steady-state scenario. To determine horizontal strain rates independently, we used data from eight markers located along a circle with a 2 km radius around the dome. The markers were positioned using differential GPS in 2012 and 2013 (Drews et al., 2015). The horizontal strain rates ($\dot{\varepsilon}_{xx} + \dot{\varepsilon}_{yy}$) were calculated to be $2 \times 10^{-3}\,a^{-1}$. Mass conservation then gives a vertical strain rate at the surface of $-2 \times 10^{-3}\,a^{-1}$. The shape of the vertical velocity profile was then used and scaled to match this value with the long-term SMB of $0.55\,m\,a^{-1}$ ice equivalent (Fig. 2). The second model, based on Dansgaard–Johnsen (D–J), was used to fit the characteristics of the Raymond effect at the ice divide. Assuming that the horizontal velocity here is zero, the vertical velocity is maximum at the surface, given by the SMB (with negative sign), and is zero at the bed. Assuming a vertical strain rate of $-2 \times 10^{-3}\,a^{-1}$ at the surface, we can determine the kink point (between constant strain rate above and a strain rate linearly decreasing with depth below) that obeys these conditions (Cuffey and Paterson, 2010). This approach indicates that the kink point lies at $0.9\,H$, where H is the ice thickness. As seen in Fig. 2b, this method yields a vertical strain pattern that is consistent with that of Drews et al. (2015), especially in the first 120 m corresponding to the length of the ice core.

We calculate annual layer thickness, and consequent SMB, using vertical strain rates determined by both the Drews and the D–J methods. Annual layer thicknesses were then converted from ice equivalent to water equivalent to facilitate comparison with other studies.

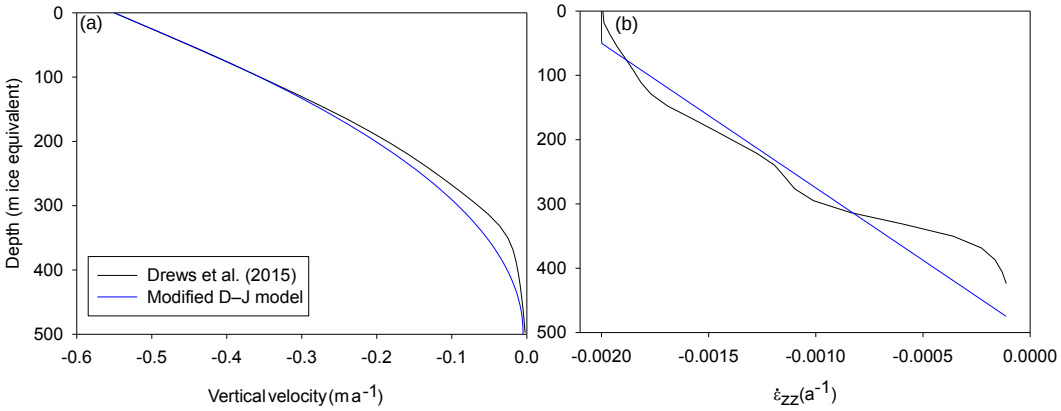

Figure 2. (a) Vertical velocity profiles and **(b)** vertical strain-rate profiles according to the modified Dansgaard–Johnsen model (blue) and the full Stokes model (black; Drews et al., 2015).

2.5 Community Earth System Model (CESM)

Atmospheric reanalyses (ERA-Interim; Dee and Uppala, 2009) and regional climate models are compared to the ice core SMB in Sect. 3.4. These models extend back to 1979, covering only a small proportion of the ice core record. Thus, to interpret our ice-core-derived SMB record and relate it to large-scale climate conditions, we use SMB, sea ice, and temperature output from the Community Earth System Model (CESM). CESM is a global, fully coupled, CMIP6-generation climate model with an approximate horizontal resolution of 1°, and has recently been used successfully to simulate present-day Antarctic climate and SMB (Lenaerts et al., 2016). Because CESM is not bound by observations, and is a freely evolving model that generates its own climate, the simulated SMB time series cannot be directly compared to the observed one. Instead we use a statistical approach: we use the historical time series of CESM (156 years, 1850–2005) that overlaps with most of the ice core record, and group the 16 single years (i.e. $\sim 10\,\%$) with the highest SMB and lowest SMB in that time series. We take the mean SMB of the ice-covered CESM grid points of the coastal region around the ice core (20–30° E, 69–72° S) as a representative value. For the grouped years of highest and lowest SMB, we take the anomalies (relative to the 1850–2005 mean) in near-surface temperature and sea-ice fraction as parameters to describe the regional ocean and atmosphere conditions corresponding to these extreme years. The sea-ice extent simulated by CESM during the observational period matches observations closely (Lenaerts et al., 2016) and does not show any temporal trend in the Atlantic sector, providing confidence that the model treats sea ice realistically.

3 Results

3.1 Dating

3.1.1 Relative dating (seasonal peak counting)

Annual layers are identified on the basis of high-resolution water stable isotopes (δ^{18}O, δD), smoothed ECM, chemical species, and their ratios (Figs. 3, S1 and S2). While all of these physico-chemical properties generally show a clear seasonality, they also change smoothly over the few very thin ice layers identified in the core (white dots in Fig. 3), indicating that they are not disturbed by surface melting. The summer peak in water stable isotopes is obvious in most cases. The boundary between annual layers was identified as the middle depth of the peak above the mean δ^{18}O value (thin black line in Fig. 3), considered as the "summer season". Major ions such as $nss\mathrm{SO_4}$, $\mathrm{NO_3^-}$, and especially the ratio $\mathrm{Na^+}$ / $\mathrm{SO_4^=}$, generally help to distinguish ambiguous peaks in the isotopic record. $\mathrm{SO_4^=}$ is one of the oxidation products of dimethyl sulfide (DMS), a degradation product of DMSP (dimethylsulfoniopropionate), which is synthesized by sea ice microorganisms (sympagic) as an antifreeze and osmotic regulator (e.g. Levasseur, 2013). Both $nss\mathrm{SO_4}$ and $\mathrm{Na^+}$ / $\mathrm{SO_4^=}$ vary seasonally. $\mathrm{NO_3^-}$ also shows a seasonal signal, but the processes controlling its seasonality are not yet fully understood (Wolff et al., 2008). For ECM, there is also a regular seasonal signal, which is sometimes blurred below 80 m, although some seasonal cycles can still be seen, between 115 and 118 m (Fig. S2), for example. Two extreme age–depth profiles (youngest and oldest) resulted from this counting procedure, taking the remaining ambiguities into account (Fig. S2). The mean age–depth profile is presented in Fig. 4 with the ranges associated with the two extreme age–depth estimates. Between 237 and 269 annual cycles were identified between the reference surface (November AD 2012) and the bottom of the core, which is correspond-

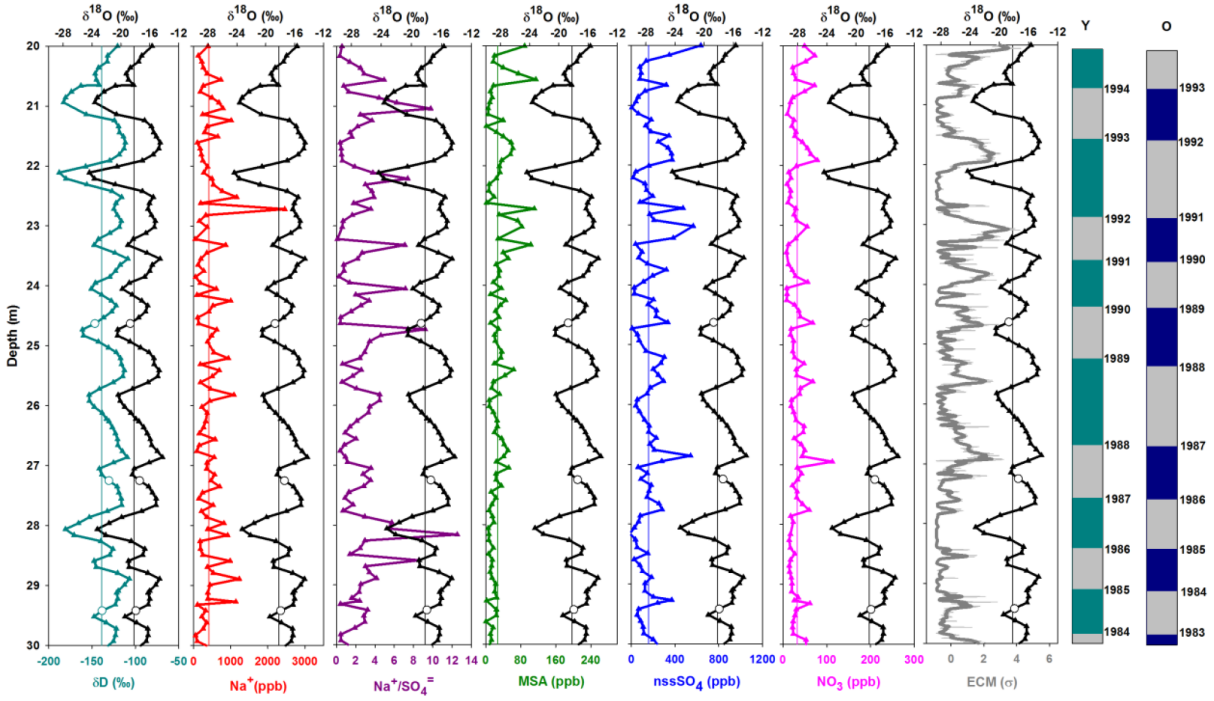

Figure 3. A 10 m-long illustrative example of how variations in stable isotopes (δ^{18}O, δD), chemical species (or their ratios), and smoothed ECM (running mean, 0.1 m) are used to identify annual layers. Coloured bars on the right indicate the annual layer boundaries (middle depth of each period corresponding to above average δ^{18}O values) for the youngest (Y) and oldest (O) estimates, with 1-year difference at 20 m depth. See Figs. S1 and S2 for the whole profile. White dots in the δ^{18}O and δD profiles indicate thin ice layers identified visually in the core. δ^{18}O profiles are shown multiple times to better illustrate correlations between δ^{18}O and other profiles.

ingly dated to AD 1775 and 1743 respectively, with a mean age of AD 1759 ± 16.

In the oldest estimate, each $Na^+ / SO_4^=$ can generally be associated with a δ^{18}O minimum, even in the deep parts of the record. This is the case between 101 and 110 m or between 112 and 115 m, for example (Fig. S2), while in the youngest estimate, these years show a double peak in $Na^+ / SO_4^=$, suggesting the latter underestimates the number of years. This age–depth range may be evaluated further on the basis of identifying volcanic signals in the core's ECM record.

3.1.2 Refinement of the age–depth scale on the basis of volcanic horizons

Volcanic indicators (ECM, *nss*SO_4, $SO_4^= / Na^+$) can potentially be used to identify specific, dated volcanic eruptions, allowing us to reduce the uncertainties resulting from the relative dating procedure. However, the unambiguous identification of eruptions is challenging in ice cores from coastal regions, where the ECM and *nss*SO_4 background signals are commonly highly variable due to the proximity of the ocean and ocean-related MSA products (Fig. S1). Given our preliminary relative core-based date of AD 1759 ± 16 (Sect. 3.1.1 above), we searched our ECM record for vol-

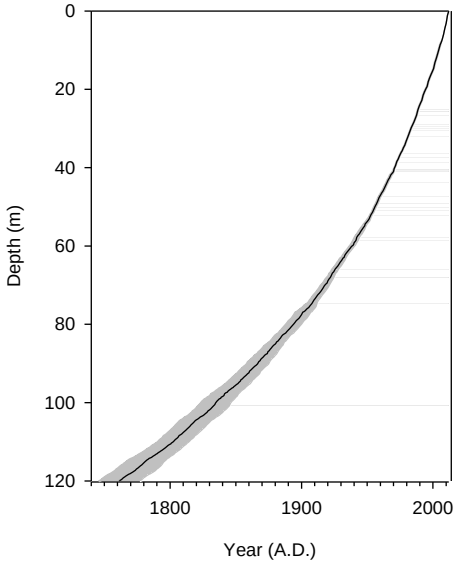

Figure 4. Age–depth relationship for IC12 reconstructed from the relative dating process. Grey shading shows the uncertainty range between the oldest and the youngest estimates. The uncertainty range reaches a maximum of ±16 years at the base of the core.

Table 1. Mean SMB at IC12 for different time periods. These values may be compared with those of several published studies, summarized in Table S1.

Period (years AD)	SMB (m w.e. a^{-1}) (oldest estimate)	SMB (m w.e. a^{-1}) (youngest estimate)	Mean SMB (m w.e. a^{-1})
1816–2011	0.476	0.513	0.495
1816–1900	0.401	0.441	0.421
1900–2011	0.532	0.568	0.550
1816–1961	0.432	0.476	0.454
1962–2011	0.604	0.623	0.614
1816–1991	0.459	0.498	0.479
1992–2011	0.626	0.651	0.638

canic horizons of known ages that fell within our relative age range. The best match here is provided by our oldest age–depth scale (Philippe et al., 2016a), with the major Tambora eruption seeming to appear at 102.35 m (Fig. 5). Here, the peak in our ECM record exceeds 4σ, while an adjacent earlier peak, exceeding 2σ, may be attributed to an eruption from an unknown volcano in 1809 (Traufetter et al., 2004). Although these ECM responses are less pronounced than in other inland cores such as at West Antarctic Ice Sheet divide (Sigl et al., 2013), a 2σ threshold is commonly considered as sufficient evidence for a match to volcanic eruptions (e.g. Kaczmarska et al., 2004) and allows potential matching of 13 volcanoes within our record. However, several other peaks above 2σ could not be associated with any known volcanic eruption. Given this uncertainty, we conclude that the core's ECM record is too noisy for our age–depth scale to be refined with confidence by matching to volcanic eruptions. We therefore keep both estimates resulting from our layer-count-based dating process and use them as an indication of the influence of dating uncertainty on our SMB reconstruction.

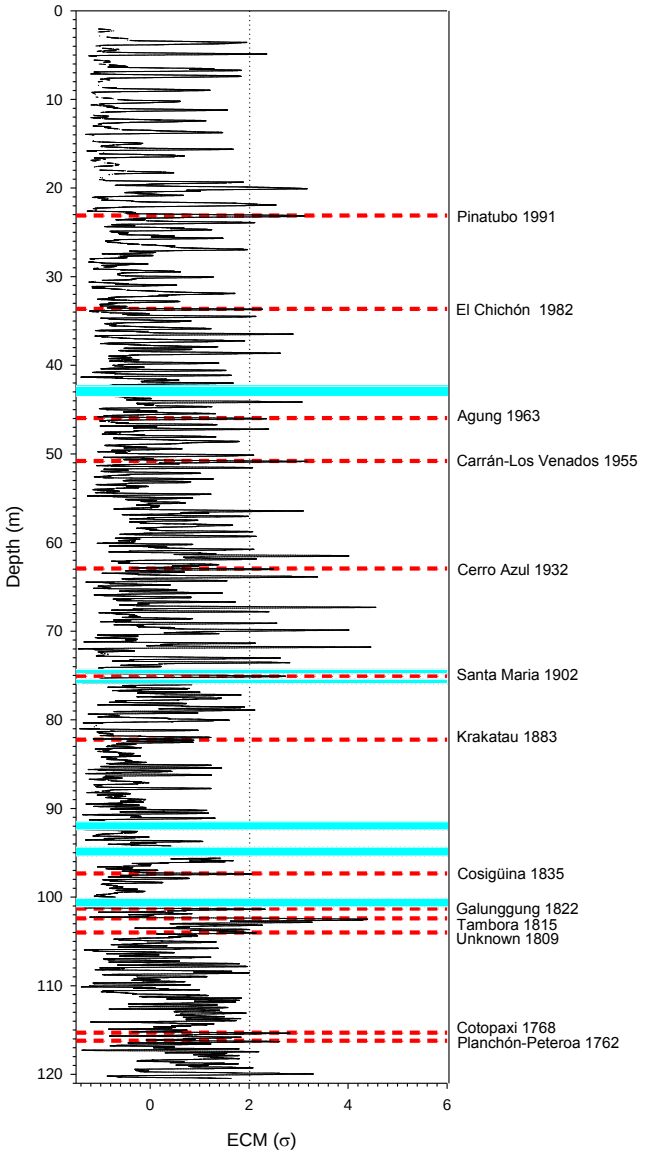

Figure 5. Continuous record of ECM (except for six measurement gaps shown as cyan bands). Normalized conductivity (black line) is expressed as a multiple of standard deviation (σ). The 2σ threshold is shown as a dotted vertical line, and identified volcanic peaks are shown as dashed red horizontal lines.

3.2 Surface mass balance record

Combining annual layer thickness data with gravimetric density best fit (Hubbard et al., 2013) and thinning rate corrections, we reconstructed the SMB record at the DIR summit from AD 1759 ± 16 years to November 2012 (Fig. 6). Without correction for layer thinning, the mean annual layer thickness is 0.36 ± 0.02 m w.e. This is compared with the reconstructed record of SMB including corrections for thinning, via Drews and D–J (Sect. 2.4 above) in Fig. 6a. Both corrections are undistinguishable. Since the correction based on Drews et al. (2015) is more closely guided by field measurements than the modified D–J model, we henceforth consider only the record corrected by Drews. Figure 6b and c show the oldest and the youngest estimates respectively and include an 11-year running mean applied to reduce interannual variability. Error bars are derived from the 5–10 cm depth uncertainty on annual layer thickness, depending on the water stable isotopes resolution, and converted to m w.e. The uncertainty range drawn in Fig. 6d is bounded by the oldest and youngest estimates. The mean SMB for the whole period is 0.47 ± 0.02 m w.e., ranging between 0.26 ± 0.01 and 1 ± 0.03 m w.e. All curves also show a clear positive trend in SMB from at least the second half of the 20th century.

We define four different SMB time periods (summarized in Table 1) beginning from 1816 because of the Tambora marker (allowing comparison with other studies, Table S1), and because confidence is reduced by the decreasing signal-to-noise ratio before this. As the ice core was recovered in November 2012, that incomplete year is not included

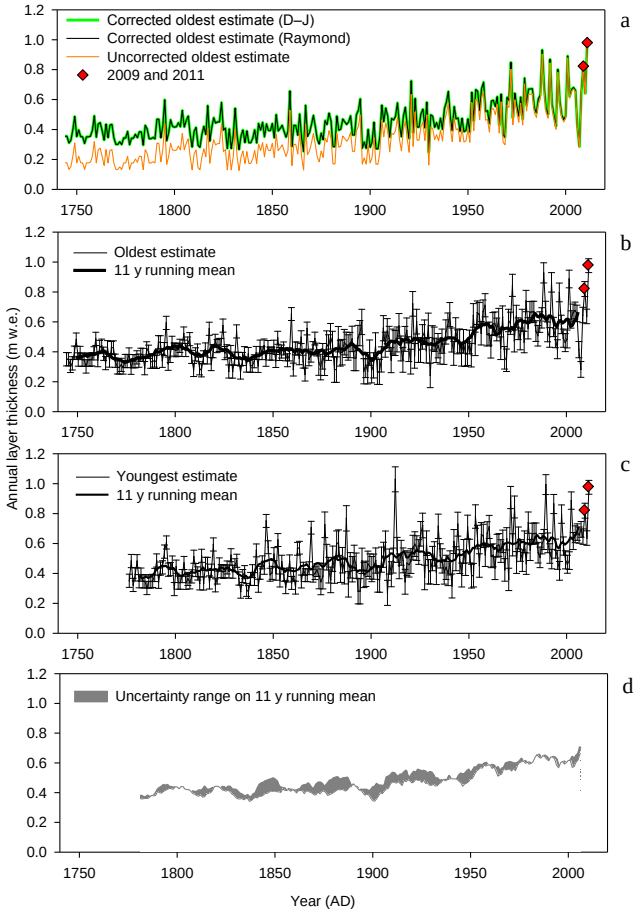

Figure 6. Annual layer thicknesses at IC12 in m w.e. **(a)** For the oldest estimate: uncorrected annual layer thickness (orange line), corrected annual layer thickness using the full Stokes (Drews et al., 2015) model (black line), and corrected annual layer thickness with the modified Dansgaard–Johnsen model (green line, undistinguishable from the black line at this scale); **(b)** corrected annual layer thickness using Drews et al. (2015) model with error bars, showing 5–10 cm depth uncertainty (thin black line) and 11 year running mean (thick black line) for the oldest estimate; **(c)** same as **(b)** but for the youngest estimate; **(d)** range of uncertainty between youngest and oldest estimates (11 year running mean). Red diamonds highlight years 2009 and 2011, discussed in the text.

in the summaries. These periods are (i) the full 195-year time period (1816 to 2011), (ii) the last 111 years relative to the previous full time period (i.e. 1900–2011 vs. 1816–1900), (iii) the last 50 years relative to the previous full time period (i.e. 1962–2011 vs. 1816–1961), and (iv) the last 20 years relative to the previous full time period (i.e. 1992–2011 vs. 1816–1992). For the full 195-year time period (1816 to 2011), the mean SMB, including correction for layer thinning, is 0.49 ± 0.02 m w.e. a^{-1}. For the last 111 years (1900–2011), the SMB is 0.55 ± 0.02 m w.e. a^{-1}, representing a 26 ± 1 % increase compared to the previous period. For the last 50 years (1962–2011), the SMB is 0.61 ± 0.01 m w.e. a^{-1}, representing a 32 ± 4 % increase compared to the previous period. For the last 20 years (1992–2011), the SMB is 0.64 ± 0.01 m w.e. a^{-1}, representing a 32 ± 3 % increase compared to the previous period.

Detailed annual SMBs reconstructed for the last 10 years for our oldest and youngest estimates are summarized in Table 2. These records indicate recent SMB values that fall at the top end of those reconstructed throughout the period 1816–2011. For the oldest estimate, the highest SMB during the last 10 years occurred in 2011, followed by 2009. With values of 0.98 and 0.82 m w.e. a^{-1}, these fall within the 1 and 2 % highest SMB years of the whole record ($\sim$ 250 years) respectively. For the youngest estimate, the highest SMB during the last 10 years occurred in 2011, followed closely by 2002 and 2009. With values of 0.98, 0.89, and 0.82 m w.e. a^{-1}, these fall within the 1, 2, and 3 % highest SMB years of the whole record respectively.

3.3 Sources of uncertainty

Surface mass balance reconstructed from ice cores can be characterized by substantial uncertainty (Rupper et al., 2015). The accuracy of reconstructed SMB depends on the dating accuracy, which in our case is bounded by the oldest and youngest estimates. Also, given our vertical sampling resolution of $\delta^{18}O$, the location of summer peaks is only identifiable to a precision of 0.05 m where no other data are available. However, our multi-parameter records (Figs. 3 and S1) indicate that annual layer thickness throughout the core's full length (and particularly since $\sim$ 1815, the time period we focus on) is greater than our sample length, providing confidence that we are not missing annual layers that are thinner than our samples. Our belief that $\delta^{18}O$ cycles demarcate annual layers throughout the record is further supported by the one-to-one correspondence between this parameter and the Na^+ / $SO_4^=$ ratio, even in the deepest part of the core.

SMB reconstructions are also influenced by density measurement error ($\sim$ 2 % herein) and small-scale variability in densification. However, the influence of this effect on SMB is very small. For example, Callens et al. (2016) used a semi-empirical model of firn compaction (Arthern et al., 2010), adjusting parameters to fit the discrete measurements instead of using the best fit from Hubbard et al. (2013). Applying the model of Callens et al. (2016) to our data results in reconstructed SMB mean values that differ by less than 2 % from our analysis based on Hubbard et al. (2013).

Vertical strain rates also represent a potential source of error. A companion paper (Philippe et al., 2016b) will be dedicated to a more precise assessment of this factor using repeated borehole optical televiewer stratigraphy. However, the present study uses a field-validated strain rate model and shows that using the simpler modified Dansgaard–Johnsen model changes the reconstructed SMB by a maximum of 0.001 m w.e. a^{-1}. Therefore, we are confident that refining the strain rate profile will not change our main conclusions.

Temporal variability of SMB at certain locations can also be due to the presence of surface undulations upstream (e.g. Kaspari et al., 2004), but this effect is minimized at ice divides.

Another possible source of error is the potential migration of the crest. Indeed, radar layers show SMB asymmetry next to the DIR crest. Although the crest of DIR must have remained laterally stable for thousands of years or more to explain the comparatively large Raymond arches in the ice stratigraphy (Drews et al., 2013; Callens et al., 2016), we cannot exclude a recent crest migration over the last decades, particularly because the lateral offset of the SMB maximum towards the upwind side (inferred from the radar stratigraphy) remains unexplained. However, there is twofold evidence to argue against a recent divide migration: (1) a similar offset in the SMB maximum is also found on another ice rise (Drews et al., 2013), suggesting that this offset reflects a generic pattern of atmospheric deposition near the crests rather than a recent and coincidental crest migration of two ice divides and, (2) the shallow arches in the radar stratigraphy which define the lateral offset are vertically aligned and not tilted as would be expected for a migrating divide (Drews et al., 2015; Fig. 3b).

3.4 Comparison with climate models

We compare the trend in our IC12 SMB record with outputs from three atmospheric models: ERA-Interim reanalysis (Dee et al., 2009), the CESM model (Fig. 7), and RACMO2 (Lenaerts et al., 2014). ERA-Interim shows no trend in the relatively short overlapping period (1979–2012). The ice-core-derived SMB correlates moderately to ERA-Interim and RACMO2, yielding coefficients of determination (R^2) of 0.36 and 0.5 respectively. For a longer period of overlap, we used the output of the CESM model, although it is a freely evolving model that does not allow a direct comparison with measured data. The CESM-derived average SMB at the closest grid point to DIR is too low (0.295 ± 0.061 m a^{-1}, 1850–2005), probably because the orographic precipitation effect is not well simulated. However, CESM does reproduce the general trend reconstructed from our DIR core. Subtle small-scale variations in wind speed and direction, typically not resolved by reanalyses or regional climate models, might disrupt the inter-annual variability of SMB, although we assume that it does not influence the positive SMB trend found in the ice core record. Unfortunately, our method does not allow for an explicit partitioning of the SMB explained by precipitation as opposed to wind processes. Instead, we focus on the drivers of precipitation at the ice core site using the output of CESM (Fig. 8).

In anomalously high SMB years, sea ice coverage is substantially lower than average (20–40 fewer days) with sea-ice cover, i.e. about 10–30 % reduction compared to the average of 120–200 days (Fig. 8) in the Southern Ocean northeast of the ice core location, which is the prevalent source region of atmospheric moisture for DIR (Lenaerts et al., 2013). This is associated with considerably higher near-surface temperatures (1–3 °C). In low-SMB years (not shown) we see a reverse, but less pronounced, signal with a higher sea ice fraction (10–20 days) and slightly lower temperatures at the oceanic source region of precipitation.

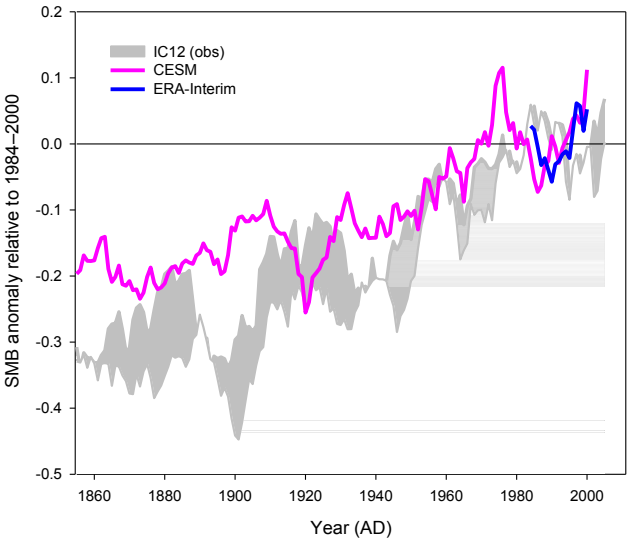

Figure 7. Comparison of SMB trends between IC12 records, with a range between youngest (upper boundary) and oldest estimate (lower boundary) shown as grey band, CESM output (pink curve), and ERA-Interim reanalysis (blue curve). All data represent anomaly relative to 1979–1989 (black line) for the overlapping period 1850–2011.

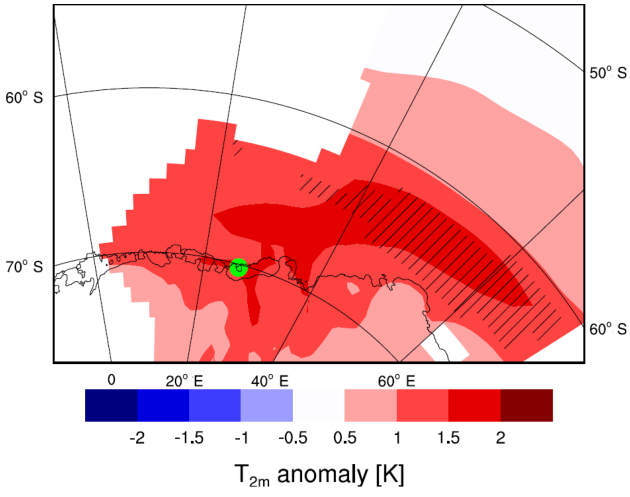

Figure 8. Large-scale atmospheric, ocean and sea-ice anomalies in high-SMB (10 % highest) years in the CESM historical time series (1850–2005). The colours show the annual mean near-surface temperature anomaly (in °C), and the hatched areas show the anomaly in sea-ice coverage (> 20 days less sea ice cover than the mean). The green dot shows the location of the ice core.

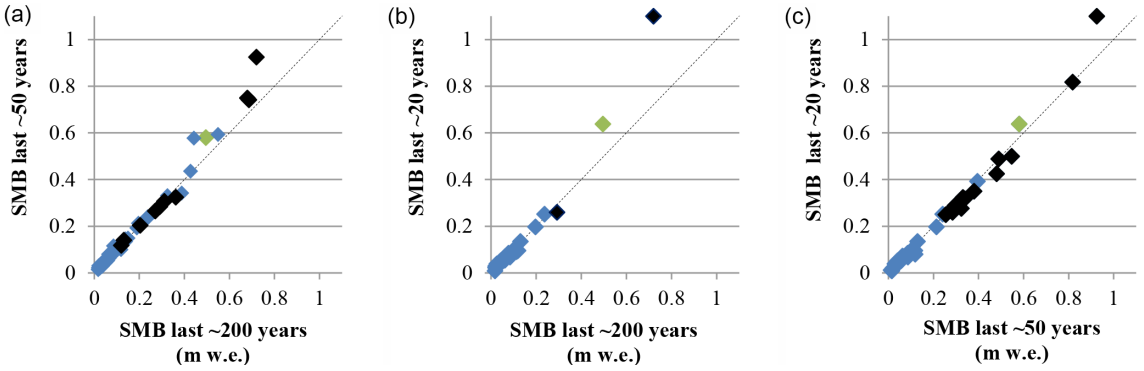

Figure 9. Comparison of SMB between different periods reconstructed for ice cores from the continent (see Table S1 for site location, references and exact periods): **(a)** the last ~200 years and the last ~50 years; **(b)** the last ~200 years and the last ~20 years; **(c)** the last ~50 years and the last ~20 years. Coastal sites (< 1500 m a.s.l. and < 100 km away from the ice shelf) are shown in black, with the exception of our study site, IC12, which is shown in green. Inland sites are shown in blue. The 1 : 1 slope (0 % change) is shown as a dotted line.

4 Discussion

4.1 Regional-scale variability

Output of the CESM shows that, along with atmospheric circulation, sea-ice cover and near-surface temperatures have an influence on precipitation at a regional scale (Fig. 8). Orography can also greatly affect SMB variability (Lenaerts et al., 2014), as can local variations in wind strength and direction. Indeed, the lower correlation between SMB derived from ERA-Interim and RACMO2 and the results of our study than with those from ice cores collected in West Antarctica (e.g. Medley et al., 2013; Thomas et al., 2015) may be explained by the strong influence of local wind-induced snow redistribution and sublimation on the wind-exposed ridge of the DIR (Lenaerts et al., 2014). However, both Drews et al. (2015) and Callens et al. (2016) showed that this spatial SMB pattern has been constant for the last few thousand of years. Therefore, our observed trend of increasing annual SMB in the ice core represents the temporal changes and is highly unlikely to be explained by a different orographic precipitation pattern caused by a change in local wind direction or strength. This argument, along with positive correlations with ERA-Interim and RACMO2 outputs, suggests that the trend we reconstruct at DIR is representative of at least the Roi Baudouin Ice Shelf, surrounding the DIR. More studies are needed in the area to confirm this inference.

4.2 Continental-scale variability

Our results show generally increasing SMB on the DIR in coastal DML over the past ~100 years. This trend continues, and possibly accelerates, up to the present. This finding is consistent with the results of large-scale modelling and climate-based studies that also indicate a SMB increase in the area (summarized in Sect. 1 above). However, until now, no increase had been detected in ice cores from the area. Our study is the first to detect in situ an increase in coastal Antarctic precipitation, which is expected to occur mainly in the peripheral areas at surface elevations below 2250 m (Krinner et al., 2007; Genthon et al., 2009).

Figure 9 shows that coastal sites (below 1500 m a.s.l. and less than 100 km from the ice shelf) do not all behave similarly. Most of the sites with high SMB (coastal or not) show an increase in SMB between the last ~50 years and the reference period (last ~200 years), whereas the sites with lower SMB show no trend, even if they are coastal (Fig. 9a). This figure also shows that only two other coastal sites can be used to compare the last ~200 years with the last 20 years (Gomez and S100, Fig. 9b and Table S1). Comparing the last ~20 years with the last ~50 years, the increase is less visible (Fig. 9c).

4.3 Causes of spatial and temporal SMB variability

The positive temporal trends and contrasts in SMB measured here and in ice cores from other areas could result from thermodynamic forcing (temperature change), dynamic forcing (change in atmospheric circulation), or both.

Higher temperature induces higher saturation vapour pressure, generally enhancing precipitation. Oerter et al. (2000) demonstrated a correlation between temperature and SMB in DML. On longer timescales (glacial–interglacial), using ice cores and models, Frieler et al. (2015) found a correlation between temperature and SMB for the whole Antarctic continent. However, both Altnau et al. (2015) and Fudge et al. (2016) found that SMB and changes in ice $\delta^{18}O$ are not always correlated. They hypothesized that changes in synoptic circulation (cyclonic activity) have more influence than thermodynamics, especially at the coast. In the presence of a blocking anticyclone at subpolar latitudes, an amplified Rossby wave induces the advection of moist air (Schlosser et al., 2010; Frezzotti et al., 2013). On these rare occasions, meridional moisture transport towards the interior of DML is

Table 2. SMB of the last 10 years from IC12 ice core (oldest and youngest estimates; see text for details).

Year (AD)	SMB (m w.e. a^{-1}) (oldest estimate)	SMB (m w.e. a^{-1}) (youngest estimate)
2011	0.980	0.980
2010	0.641	0.641
2009	0.824	0.824
2008	0.651	0.651
2007	0.287	0.699
2006	0.419	0.661
2005	0.661	0.681
2004	0.681	0.666
2003	0.666	0.621
2002	0.621	0.891

concentrated into atmospheric rivers. Two recent manifestations of these short-lived events, in 2009 and 2011, have led to a recent positive mass balance of the East Antarctic Ice Sheet (Shepherd et al., 2012; Boening et al., 2012). The effect was also recorded in situ, at a local scale, next to the Belgian Princess Elisabeth base (72° S, 21° E) (Gorodetskaya et al., 2013, 2014). Several of these precipitation events in a single year can represent up to 50 % of the annual SMB away from the coast (Schlosser et al., 2010; Lenaerts et al., 2013). At the coast, precipitation is usually event-type, but the events occur throughout the whole year. However, the 2009 and 2011 events are also observed in our data as two notably higher-than-average SMB years (Table 2). Our record places these extreme events within a historical perspective. Despite the fact that higher SMB years exist in the recent part of record, 2009 and 2011 are amongst the 2–3 % highest SMB years of the last two centuries for 2009, depending on the estimate, and 1 % for 2011.

A change in climate modes could also partly explain recent changes in SMB. The Southern Annular Mode has shifted to a more positive phase during the last 50 years (Marshall, 2003). This has led to increased cyclonic activity, but also to increased wind speed and sublimation. Kaspari et al. (2004) also established a link between periods of increased SMB and sustained El Niño events (negative Southern Oscillation Index anomalies) in 1940–1942 and 1991–1995 but our record does not support this observation.

Wind ablation represents one of the largest sources of uncertainty in modelling SMB, and is an important cause of spatial and interannual variability. Highest snowfall and highest trends in predicted snowfall are expected in the escarpment zone of the continent due to orographic uplift and the associated wind erosion (Genthon et al., 2009). For example, in the escarpment area of DML, low- to medium-sized precipitation events can be entirely removed by the wind, while high-precipitation events lead to net positive SMB (Gorodetskaya et al., 2015). An increase in SMB coupled with an increased wind speed could result in increased SMB where wind speed is low and decreased SMB where wind speed is high, which is ∼ 90 % of the Antarctic surface (Frezzotti et al., 2004). Accordingly, Frezzotti et al. (2013) suggested that SMB has increased at low-altitude sites and on the highest ridges due to more frequent anticyclonic blocking events, but has decreased at intermediate altitudes due to stronger wind ablation in the escarpment areas. In DML, however, Altnau et al. (2015) reported a SMB increase on the plateau (coupled to an increase in δ^{18}O) and a decrease on coastal sites, which they associated with a change in circulation patterns. Around Dome A, Ding et al. (2011) also reported an increase in SMB in the inland area and a recent decrease towards the coast. Their explanation is that air masses may transfer moisture inland more easily due to climate warming.

Atmospheric circulation exhibits a primary role in determining temporal and spatial SMB variability. Sea-ice and ocean surface conditions play a secondary role, and could contribute to a higher SMB in a warmer climate. A more recent study using a fully coupled climate model (Lenaerts et al., 2016) suggests that DML is the region most susceptible to an increase in snowfall in a present and future warmer climate. The snowfall increase in the coastal regions is particularly attributed to loss of sea ice cover in the southern Atlantic Ocean, which in turn enhances atmospheric moisture uptake by evaporation. This is further illustrated in Fig. 8, which suggests that extremely high SMB years are associated with low sea ice cover. The longer exposure of open water leads to higher near-surface temperatures and enhances evaporation and moisture availability for ice sheet precipitation (Lenaerts et al., 2016).

5 Conclusions

A 120 m-long ice core was drilled on the summit of the DIR, and dated to AD 1759 ± 16 using δ^{18}O, δD, major ion, and ECM data. Due to the coastal location of the ice core, the identification of volcanic horizons in the ECM record is hampered by high background acidity. Therefore, we counted annual layers to develop oldest and youngest age–depth estimates. We combine annual layer thickness with density and thinning functions to calculate SMB time series from the core. The mean SMB for the period 1816–2011 is 0.47 ± 0.02 m w.e. a^{-1}, which increases for more recent time periods such that mean SMB for the past 20 years (1991–2011) rises by 32 ± 3 % to 0.64 ± 0.01 m w.e. a^{-1}. This supports the trend calculated by the CESM for the area. Wind redistribution is significant near the ice core location, but this effect appears to have been temporally uniform, giving confidence that the SMB changes we report represent temporal change rather than the effects of local migration in the spatial pattern of SMB.

SMB trends observed in other records across Antarctica are spatially highly variable. In coastal East Antarctica, our

study is the only one to show an increase in SMB during the past ~ 100 years. Many studies point to a difference in the behaviour of coastal and inland sites, due to a combination of thermodynamics and dynamic processes. A combination of spatial variability in snowfall and snow redistribution by the wind likely explains much of this observed spatial variability. Neither currently available climate models nor reanalysis data are able to resolve ice-rise topography, which makes detailed predictions from these methods difficult to match to our ice-core-derived SMB time series. Nevertheless, their temporal trends broadly match those of our reconstructed SMB, and the comparison suggests that SMB variability is governed to a large extent by atmospheric circulation and to a lesser extent by variations in sea ice cover. More studies are needed at other coastal sites in East Antarctica to determine how representative this result and our interpretations are.

Long time series of annual SMB are scarce in coastal East Antarctica. The summit of the Derwael Ice Rise represents a suitable site for deep drilling. It has a relatively high SMB, clear annual layering, and appropriate ice conditions (few thin ice layers) for paleoclimate reconstruction. According to the full Stokes model (Drews et al., 2015), drilling to 350 m could reveal at least 2000 years of a reliable climate record at high resolution, which would address one of the priority targets ("IPICS-2k array"; Steig et al., 2005) of the International Partnership in Ice Core Sciences (IPICS).

6 Data availability

Annual layer thicknesses and age–depth data are available online (doi:10.1594/PANGAEA.857574, Philippe et al., 2016a).

The Supplement related to this article is available online at doi:10.5194/tc-10-2501-2016-supplement.

Acknowledgements. This paper forms a contribution to the Belgian Research Programme on the Antarctic (Belgian Federal Science Policy Office), Project SD/SA/06A "Constraining ice mass changes in Antarctica" (IceCon). The authors wish to thank the International Polar Foundation for logistic support in the field. Morgane Philippe is partly funded by a grant from Fonds David et Alice Van Buuren. Jan T. M. Lenaerts is funded by Utrecht University through its strategic theme "Sustainability", sub-theme "Water, Climate and Ecosystems", and the programme of the Netherlands Earth System Science Centre (NESSC), financially supported by the Ministry of Education, Culture and Science (OCW). Philippe Claeys thanks the Hercules Foundation (www.herculesstichting.be/) for financing the upgrade of the stable isotope laboratory. Reinhard Drews was supported by the Deutsche Forschungsgemeinschaft (DFG) in the framework of the priority programme "Antarctic Research with comparative investigations in Arctic ice areas" by the grant MA 3347/10-1. The research leading to these results received funding from the European Research Council under the European Community's Seventh Framework Programme (FP7/2007-2013)/ERC grant agreement 610055 as part of the Ice2Ice project. Ice coring equipment benefitted from an Aberystwyth University Capital Infrastructure grant and the optical televiewer data from NERC grant NE/J013544/1. The authors thank Irina Gorodetskaya for her helpful comments and the Norwegian Polar Institute for developing Quantarctica and making this GIS package for Antarctica freely available. The initial version of the article benefited from the very constructive comments and corrections of the two anonymous referees and the editor.

Edited by: K. Matsuoka
Reviewed by: two anonymous referees

References

Altnau, S., Schlosser, E., Isaksson, E., and Divine, D.: Climatic signals from 76 shallow firn cores in Dronning Maud Land, East Antarctica, The Cryosphere, 9, 925–944, doi:10.5194/tc-9-925-2015, 2015.

Anschütz, H., Sinisalo, A., Isaksson, E., McConnell, J. R., Hamran, S.-E., Bisiaux, M. M., Pasteris, D., Neumann, T. A., and Winther, J.-G.: Variation of accumulation rates over the last eight centuries on the East Antarctic Plateau derived from volcanic signals in ice cores, J. Geophys. Res., 116, D20103, doi:10.1029/2011JD015753, 2011.

Aristarain, A. J., Delmas, R. J., and Stievenard, M.: Ice-core study of the link between sea-salt aerosol, sea-ice cover and climate in the Antarctic Peninsula area, Clim. Change, 67, 63–86, doi:10.1007/s10584-004-0708-6, 2004.

Arthern, R. J., Vaughan, D. G., Rankin, A. M., Mulvaney, R., and Thomas, E. R.: In situ measurements of Antarctic snow compaction compared with predictions of models, J. Geophys. Res., 115, F03011, doi:10.1029/2009JF001306, 2010.

Boening, C., Lebsock, M., Landerer, F., and Stephens, G.: Snowfall driven mass change on the East Antarctic ice sheet, Geophys. Res. Lett., 39, L21501, doi:10.1029/2012GL053316, 2012.

Bromwich, D. H., Nicolas, J. P., and Monaghan, A. J.: An assessment of precipitation changes over Antarctica and the Southern Ocean since 1989 in contemporary global reanalyses, J. Clim., 24, 4189–4209, doi:10.1175/2011jcli4074.1, 2011.

Bromwich, D. H., Nicolas, J. P., Monaghan, A. J., Lazzara, M. A., Keller, L. M., Weidner, G. A., and Wilson, A. B.: Corrigendum: Central West Antarctica among the most rapidly warming regions on Earth, Nat. Geosci., 7, 76–76, doi:10.1038/ngeo2016, 2014.

Callens, D., Drews, R., Witrant, E., Philippe, M., and Pattyn, F.: Temporally stable surface mass balance asymmetry across an ice rise derived from radar internal reflection horizons through inverse modeling, J. Glaciol., 1, 1–10, doi:10.1017/jog.2016.41, 2016.

Cuffey, K. M. and Paterson, W.: The Physics of Glaciers, Elsevier, 693 pp., doi:10.1016/c2009-0-14802-x, 2010.

Dansgaard, W. and Johnsen, S.: A flow model and a time scale for the ice core from Camp Century, Greenland, J. Glaciol., 8, 215–223, 1969.

Davis, C. H., Li, Y., McConnell, J. R., Frey, M. M., and Hanna, E.: Snowfall-driven growth in East Antarctic Ice Sheet mitigates recent sea-level rise, Science, 308, 1898–1901, doi:10.1126/science.1110662, 2005.

Dee, D. P. and Uppala, S. M.: Variational bias correction of satellite radiance data in the ERA-Interim reanalysis, Q. J. Roy. Meteorol. Soc., 135, 1830–1841, doi:10.1002/qj.493, 2009.

Ding, M., Xiao, C., Li, Y., Ren, J., Hou, S., Jin, B., and Sun, B.: Spatial variability of surface mass balance along a traverse route from Zhongshan station to Dome A, Antarctica, J. Glaciol., 57, 658–666, doi:10.3189/002214311797409820, 2011.

Drews, R., Steinhage, D., Martín, C., and Eisen, O.: Characterization of glaciological conditions at Halvfarryggen ice dome, Dronning Maud Land, Antarctica, J. Glaciol., 59, 9–20, doi:10.3189/2013JoG12J134, 2013.

Drews, R., Matsuoka, K., Martín, C., Callens, D., Bergeot, N., and Pattyn, F.: Evolution of Derwael Ice Rise in Dronning Maud Land, Antarctica, over the last millennia, J. Geophys. Res.-Earth, 120, 564–579, doi:10.1002/2014JF003246, 2015.

Fernandoy, F., Meyer, H., Oerter, H., Wilhelms, F., Graf, W., and Schwander, J.: Temporal and spatial variation of stable-isotope ratios and accumulation rates in the hinterland of Neumayer station, East Antarctica, J. Glaciol., 56, 673–687, doi:10.3189/002214310793146296, 2010.

Frezzotti, M., Pourchet, M., Flora, O., Gandolfi, S., Gay, M., Urbini, S., Vincent, C., Becagli, S., Gragnani, R., Proposito, M., Severi, M., Traversi, R., Udisti, R., and Fily, M.: New estimations of precipitation and surface sublimation in East Antarctica from snow accumulation measurements, Clim. Dynam., 23, 803–813, doi:10.1007/s00382-00004-00462-0038500803-00813, 2004.

Frezzotti, M., Pourchet, M., Flora, O., Gandolfi, S., Gay, M., Urbini, S., Vincent, C., Becagli, S., Gragnani, R., Proposito, M., Severi, M., Traversi, R., Udisti, R., and Fily, M.: Spatial and temporal variability of snow accumulation in East Antarctica from traverse data, J. Glaciol., 51, 113–124, doi:10.3189/172756505781829502, 2005.

Frezzotti, M., Scarchilli, C., Becagli, S., Proposito, M., and Urbini, S.: A synthesis of the Antarctic surface mass balance during the last 800 yr, The Cryosphere, 7, 303–319, doi:10.5194/tc-7-303-2013, 2013.

Frieler, K., Clark, P. U., He, F., Buizert, C., Reese, R., Ligtenberg, S. R., van den Broeke, M. R., Winkelmann, R., and Levermann, A.: Consistent evidence of increasing Antarctic accumulation with warming, Nat. Clim. Change, 5, 348–352, doi:10.1038/nclimate2574, 2015.

Fudge, T. J., Markle, B. R., Cuffey, K. M., Buizert, C., Taylor, K. C., Steig, E. J., Waddington, E. D., Conway, H., and Koutnik, M.: Variable relationship between accumulation and temperature in West Antarctica for the past 31,000 years, Geophys. Res. Lett., 43, 3795–3803, doi:10.1002/2016GL068356, 2016.

Fujita, S., Holmlund, P., Andersson, I., Brown, I., Enomoto, H., Fujii, Y., Fujita, K., Fukui, K., Furukawa, T., Hansson, M., Hara, K., Hoshina, Y., Igarashi, M., Iizuka, Y., Imura, S., Ingvander, S., Karlin, T., Motoyama, H., Nakazawa, F., Oerter, H., Sjöberg, L. E., Sugiyama, S., Surdyk, S., Ström, J., Uemura, R., and Wilhelms, F.: Spatial and temporal variability of snow accumulation rate on the East Antarctic ice divide between Dome Fuji and EPICA DML, The Cryosphere, 5, 1057–1081, doi:10.5194/tc-5-1057-2011, 2011.

Genthon, C., Krinner, G., and Castebrunet, H.: Antarctic precipitation and climate-change predictions: horizontal resolution and margin vs plateau issues, Ann. Glaciol., 50, 55–60, doi:10.3189/172756409787769681, 2009.

Gorodetskaya, I. V., Van Lipzig, N. P. M., Van den Broeke, M. R., Mangold, A., Boot, W., and Reijmer, C. H.: Meteorological regimes and accumulation patterns at Utsteinen, Dronning Maud Land, East Antarctica: Analysis of two contrasting years, J. Geophys. Res.-Atmos., 118, 1700–1715, doi:10.1002/jgrd.50177, 2013.

Gorodetskaya, I. V., Tsukernik, M., Claes, K., Ralph, M. F., Neff, W. D., and Van Lipzig, N. P. M.: The role of atmospheric rivers in anomalous snow accumulation in East Antarctica, Geophys. Res. Lett., 41, 6199–6206, doi:10.1002/2014GL060881, 2014.

Gorodetskaya, I. V., Kneifel, S., Maahn, M., Van Tricht, K., Thiery, W., Schween, J. H., Mangold, A., Crewell, S., and Van Lipzig, N. P. M.: Cloud and precipitation properties from ground-based remote-sensing instruments in East Antarctica, The Cryosphere, 9, 285–304, doi:10.5194/tc-9-285-2015, 2015.

Hammer, C. U.: Acidity of polar ice cores in relation to absolute dating, past volcanism, and radio-echoes, J. Glaciol., 25, 359–372, doi:10.3198/1980JoG25-93-359-372, 1980.

Hammer, C. U., Clausen, H. B., and Langway Jr., C. C.: Electrical conductivity method (ECM) stratigraphic dating of the Byrd Station ice core, Antarctica, Ann. Glaciol., 20, 115–120, doi:10.3189/172756409787769681, 1994.

Hofstede, C. M., van de Wal, R. S. W., Kaspers, K. A., van den Broeke, M. R., Karlöf, L., Winther, J. G., Isaksson, E., Lappegard, G., Mulvaney, R., Oerther, H., and Wilhelms, F.: Firn accumulation records for the past 1000 years on the basis of dielectric profiling of six firn cores from Dronning Maud Land, Antarctica, J. Glaciol., 50, 279–291, doi:10.3189/172756504781830169, 2004.

Hubbard, B., Tison, J.-L., Philippe, M., Heene, B., Pattyn, F., Malone, T., and Freitag, J. J.: Ice shelf density reconstructed from optical televiewer borehole logging, Geophys. Res. Lett., 40, 5882–5887, doi:10.1002/2013gl058023, 2013.

Isaksson, E. and Melvold, K.: Trends and patterns in the recent accumulation and oxygen isotope in coastal Dronning Maud Land, Antarctica: interpretations from shallow ice cores, Ann. Glaciol., 35, 175–180, doi:10.3189/172756402781817356, 2002.

Isaksson, E., Karlén, W., Gundestrup, N., Mayewski, P., Whitlow, S., and Twickler, M.: A century of accumulation and temperature changes in Dronning Maud Land, Antarctica, J. Geophys. Res., 101, 7085–7094, doi:10.1029/95jd03232, 1996.

Isaksson, E., van den Broeke, M. R., Winther, J.-G., Karlöf, L., Pinglot, J. F., and Gundestrup, N.: Accumulation and proxytemperature variability in Dronning Maud Land, Antarctica, determined from shallow firn cores, Ann. Glaciol., 29, 17–22, doi:10.3189/172756499781821445, 1999.

ISMASS Committee: Recommendations for the collection and synthesis of Antarctic Ice Sheet mass balance data, Global Planet. Change, 42, 1–15, doi:10.1016/j.gloplacha.2003.11.008, 2004.

Kaczmarska, M., Isaksson, E., Karlöf, K., Winther, J.-G., Kohler, J., Godtliebsen, F., Ringstad Olsen, L., Hofstede, C. M., van den Broeke, M. R., Van DeWal, R. S. W., and Gundestrup, N.:

Accumulation variability derived from an ice core from coastal Dronning Maud Land, Antarctica, Ann. Glaciol., 39, 339–345, doi:10.3189/172756404781814186, 2004.

Karlöf, L., Winther, J. G., Isaksson, E., Kohler, J., Pinglot, J. F., Wilhelms, F., Hansson, M., Holmlund, P., Nyman, M., Pettersson, R., Stenberg, M., Thomassen, M. P. A., van der Veen, C., and van de Wal, R. S. W.: A 1500 year record of accumulation at Amundsenisen western Dronning Maud Land, Antarctica, derived from electrical and radioactive measurements on a 120 m ice core, J. Geophys. Res., 105, 12471–12483, doi:10.1029/1999JD901119, 2000.

Karlöf, L., Isakson, E., Winther, J. G., Gundestrup, N., Meijer, H. A. J., Mulvaney, R., Pourcher, M., Hofstede, C., Lappegard, G., Petterson, R., van den Broecke, M. R., and van de Wal, R. S. W.: Accumulation variability over a small area in east Dronning Maud Land, Antarctica, as determined from shallow firn cores and snow pits: some implications for ice, J. Glaciol., 51, 343–352, doi:10.3189/172756505781829232, 2005.

Kaspari, S., Mayewski, P. A., Dixon, D. A., Spikes, V. B., Sneed, S. B., Handley, M. J., and Hamilton, G. S.: Climate variability in west Antarctica derived from annual accumulation-rate records from ITASE firn/ice cores, Ann. Glaciol., 39, 585–594, doi:10.3189/172756404781814447, 2004.

King, M. A., Bingham, R. J., Moore, P., Whitehouse, P. L., Bentley, M. J., and Milne, G. A.: Lower satellite-gravimetry estimates of Antarctic sea-level contribution, Nature, 491, 586–589, doi:10.1038/nature11621, 2012.

Kingslake, J., Hindmarsh, R. C. A., Aðalgeirsdóttir, G., Conway, H., Corr, H. F. J., Gillet-Chaulet, F., Martín, C., King, E. C., Mulvaney, R., and Pritchard, H. D.: Full-depth englacial vertical ice sheet velocities measured using phase-sensitive radar, J. Geophys. Res.-Earth, 119, 2604–2618, doi:10.1002/2014jf003275, 2014.

Kjær, H., Vallelonga, P., Svensson, A., Elleskov, L., Kristensen, M., Tibuleac, C., Winstrup, M., and Kipfstuhl, S.: An optical dye method for continuous determination of acidity in ice cores, Environ. Sci. Technol., 50, 10485–10493, doi:10.1021/acs.est.6b00026, 2016.

Krinner, G., Magand, O., Simmonds, I., Genthon, C., and Dufresne, J. L.: Simulated Antarctic precipitation and surface mass balance at the end of the 20th and 21th centuries, Clim. Dynam. 28, 215–230, doi:10.1007/s00382-006-0177-x, 2007.

Lenaerts, J. T. M., van den Broeke, M. R., van den Berg, W. J., van Meijgaard, E., and Munneke, P. K.: A new, high resolution surface mass balance map of Antarctica (1979–2010) based on regional climate modeling, Geophys. Res. Lett., 39, L04501, doi:10.1029/2011GL050713, 2012.

Lenaerts, J. T. M., van Meijgaard, E., van den Broeke, M. R., Ligtenberg, S. R. M., Horwath, M., and Isaksson, E.: Recent snowfall anomalies in Dronning Maud Land, East Antarctica, in a historical and future climate perspective, Geophys. Res. Lett., 40, 1–5, doi:10.1002/grl.50559, 2013.

Lenaerts, J. T. M., Brownvan, J., den Broeke, M. R., Matsuoka, K., Drews, R., Callens, D., Philippe, M., Gorodetskaya, I., van Meijgaard, E., Reymer, C., Pattyn, F., and van Lipzig, N. P.: High variability of climate and surface mass balance induced by Antarctic ice rises, J. Glaciol., 60, 1101–1110, doi:10.3189/2014jog14j040, 2014.

Lenaerts, J. T. M., Vizcaino, M., Fyke, J., van Kampenhout, L., and van den Broeke, M. R.: Present-day and future Antarctic ice sheet climate and surface mass balance in the Community Earth System Model, Clim. Dynam., 47, 1367–1381, doi:10.1007/s00382-015-2907-4, 2016.

Levasseur, M.: Impact of Arctic meltdown on the microbial cycling of sulphur, Nat. Geosci., 6, 691–700, doi:10.1038/ngeo1910, 2013.

Ludescher, J., Bunde, A., Franzke, C. L., and Schellnhuber, H. J.: Long-term persistence enhances uncertainty about anthropogenic warming of Antarctica, Clim. Dynam., 46, 263–271, doi:10.1007/s00382-015-2582-5, 2015.

Magand, O., Genthon, C., Fily, M., Krinner, G., Picard, G., Frezzotti, M., and Ekaykin, A. A.: An up-to-date quality-controlled surface mass balance data set for the 90–180E Antarctica sector and 1950–2005 period, J. Geophys. Res., 112, D12106, doi:10.1029/2006JD007691, 2007.

Marshall, G. J.: Trends in the southern annular mode from observations and reanalyses, J. Climate, 16, 4134–4143, doi:10.1175/1520-0442(2003)016<4134:titsam>2.0.co;2, 2003.

Matsuoka, K., Hindmarsh, R. C., Moholdt, G., Bentley, M. J., Pritchard, H. D., Brown, J., Conway, H., Drews, R., Durand, G., Goldberg, D., Hattermann, T., Kingslake, J., Lenearts, J., Martin, C., Mulvaney, R., Nicholls, K., Pattyn, F., Ross, N., Scambos, T., and Whitehouse, P.: Antarctic ice rises and rumples: their properties and significance for ice-sheet dynamics and evolution, Earth-Sci. Rev., 150, 724–745, doi:10.1016/j.earscirev.2015.09.004, 2015.

Medley, B., Joughin, I., Das, S. B., Steig, E. J., Conway, H., Gogineni, S., Criscitiello, A. S., McConnell, J. R., Smith, B. E., van den Broeke, M. R., Lenaerts, J. T. M., Bromwich, D. H., and Nicolas, J. P.: Airborne-radar and ice-core observations of annual snow accumulation over Thwaites Glacier, West Antarctica confirm the spatiotemporal variability of global and regional atmospheric models, Geophys. Res. Lett., 40, 3649–3654, doi:10.1002/grl.50706, 2013.

Monaghan, A. J., Bromwich, D. H., Fogt, R. L., Wang, S., Mayewski, P. A., Dixon, D. A., Ekaykin, A., Frezzotti, M., Goodwin, I., Isaksson, E., Kaspari, S. D., Morgan, V. I., Oerter, H., Van Ommen, T. D., van der Veen, C. J., and Wen, J.: Insignificant change in Antarctic snowfall since the International Geophysical Year, Science, 313, 827–831, doi:10.1126/science.1128243, 2006.

Moore, J. C., Narita, H., and Maeno, N.: A continuous 770-year record of volcanic activity from East Antarctica, J. Geophys. Res., 96, 17353–17359, doi:10.1029/91jd01283, 1991.

Mosley-Thompson, E., Paskievitch, J. F., Gow, A. J., and Thompson, L. G.: Late 20th century increase in South Pole snow accumulation, J. Geophys. Res., 104, 3877–3886, doi:10.1029/1998jd200092, 1999.

Mulvaney, R., Pasteur, E. C., and Peel, D. A.: The ratio of MSA to non sea-salt sulphate in Antarctic peninsula ice cores, Tellus, 44b, 293–303, doi:10.3402/tellusb.v44i4.15457, 1992.

Nishio, F., Furukawa, T., Hashida, G., Igarashi, M., Kameda, T., Kohno, M., Motoyama, H., Naoki, K., Satow, K., Suzuki, K., Morimasa, T., Toyama, Y., Yamada, T., and Watanabe, O.: Annual-layer determinations and 167 year records of past climate of H72 ice core in east Dronning Maud Land, Antarctica,

Ann. Glaciol., 35, 471–479, doi:10.3189/172756402781817086, 2002.

Oerter, H., Graf, W., Wilhelms, F., Minikin, A., and Miller, H.: Accumulation studies on Amundsenisen, Dronning Maud Land, by means of tritium, DEP and stable isotope measurements: first results from the 1995/96 and 1996/97 field seasons, Ann. Glaciol., 29, 1–9, doi:10.3189/172756499781820914, 1999.

Oerter, H., Wilhelms, F., Jung-Rothenhausler, F., Goktas, F., Miller, H., Graf, W., and Sommer, S.: Accumulation rates in Dronning Maud Land as revealed by DEP measurements at shallow firn cores, Ann. Glaciol., 30, 27–34, doi:10.3189/172756400781820705, 2000.

Palerme, C., Genthon, C., Claud, C., Kay, J. E., Wood, N. B., and L'Ecuyer, T.: Evaluation of current and projected Antarctic precipitation in CMIP5 models, Clim. Dynam., online first, doi:10.1007/s00382-016-3071-1, 2016.

Parrenin, F., Dreyfus, G., Durand, G., Fujita, S., Gagliardini, O., Gillet, F., Jouzel, J., Kawamura, K., Lhomme, N., Masson-Delmotte, V., Ritz, C., Schwander, J., Shoji, H., Uemura, R., Watanabe, O., and Yoshida, N.: 1-D-ice flow modelling at EPICA Dome C and Dome Fuji, East Antarctica, Clim. Past, 3, 243–259, doi:10.5194/cp-3-243-2007, 2007.

Philippe, M., Tison, J.-L., Fjøsne, K., Hubbard, B., Kjær, H. A., Lenaerts, J. T. M., Drews, R., Sheldon, S. G., De Bondt, K., Claeys, P., and Pattyn, F.: Annual layer thicknesses and age-depth (oldest estimate) of Derwael Ice Rise (IC12), Dronning Maud Land, East Antarctica, doi:10.1594/PANGAEA.857574, 2016a.

Philippe, M., Hubbard, B., Pattyn, F., Fjøsne, K., Drews, R., Bruyninx, C., Bergeot, N., and Tison, J.-L.: Vertical velocities of firn and ice reconstructed from optical televiewer borehole logging at Derwael ice rise, Princess Ragnhild Coast, Antarctica, in preparation, 2016b.

Ren, J., Li, C., Hou, S., Xiao, C., Qin, D., Li, Y., and Ding, M.: A 2680 year volcanic record from the DT-401 East Antarctic ice core, J. Geophys. Res., 115, D11301, doi:10.1029/2009JD012892, 2010.

Rignot, E., Velicogna, I., van den Broeke, M. R., Monaghan, A., and Lenaerts, J.: Acceleration of the contribution of the Greenland and Antarctic ice sheets to sea level rise, Geophys. Res. Lett., 38, L05503, doi:10.1029/2011GL046583, 2011.

Rupper, S., Christensen, W. F., Bickmore, B. R., Burgener, L., Koenig, L. S., Koutnik, M. R., Miège, C., and Forster, R. R.: The effects of dating uncertainties on net accumulation estimates from firn cores, J. Glaciol., 61, 163–172, doi:10.3189/2015jog14j042, 2015.

Savitzky, A. and Golay, M. J. E.: Smoothing and Differentiation of Data by Simplified Least Squares Procedures, Anal. Chem., 36, 1627–1639, doi:10.1021/ac60214a047, 1964.

Schlosser, E. and Oerter, H.: Shallow firn cores from Neumayer, Ekströmisen, Antarctica: a comparison of accumulation rates and stable-isotope ratios, Ann. Glaciol., 35, 91–96, doi:10.3189/172756402781816915, 2002.

Schlosser, E., Manning, K. W., Powers, J. G., Duda, M. G., Birnbaum, G., and Fujita, K.: Characteristics of high-precipitation events in Dronning Maud Land, Antarctica, J. Geophys. Res., 115, D14107, doi:10.1029/2009JD013410, 2010.

Shepherd, A., Ivins, E. R., Geruo, A., Barletta, V. R., Bentley, M. J., Bettadpur, S., Briggs, K. H., Bromwich, D. H., Forsberg, R., Galin, N., Horwath, M., Jacobs, S., Joughin, I., King, M. A., Lenaerts, J. T. M., Li, J., Ligtenberg, S. R. M., Luckman, A., Luthcke, S. B., McMillan, M., Meister, R., Milne, G., Mouginot, J., Muir, A., Nicolas, J. P., Paden, J., Payne, A. J., Pritchard, H., Rignot, E., Rott, H., Sørensen, L. S., Scambos, T. A., Scheuchl, B., Schrama, E. J. O., Smith, B., Sundal, A. V., van Angelen, J. H., van de Berg, W. J., van den Broeke, M. R., Vaughan, D. G., Velicogna, I., Wahr, J., Whitehouse, P. L., Wingham, D. J., Yi, D., Young, D., and Zwally, H. J.: A reconciled estimate of ice-sheet mass balance, Science, 338, 1183–1189, doi:10.1126/science.1228102, 2012.

Sigl, M., McConnell, J. R., Layman, L., Maselli, O., McGwire, K., Pasteris, D., Dahl-Jensen, D., Steffensen, J. P., Vinther, B., Edwards, R., Mulvaney, R., and Kipfstuhl, S.: A new bipolar ice core record of volcanism from WAIS Divide and NEEM and implications for climate forcing of the last 2000 years. J. Geophys. Res.-Atmos., 118, 1151–1169, doi:10.1029/2012jd018603, 2013.

Steig, E., Fischer, H., Fisher, D., Frezzotti, M., Mulvaney, R., Taylor, K., and Wolff, E.: The IPICS 2k Array: a network of ice core climate and climate forcing records for the last two millennia, http://pages-igbp.org/download/docs/working_groups/ipics/white-papers/IPICS_2kArray.pdf (last access: 14 October 2016), IPICS (International Partnership in Ice Core Science), 2005.

Thomas, E. R., Marshall, G. J., and McConnell, J. R.: A doubling in snow accumulation in the western Antarctic Peninsula since 1850, Geophys. Res. Lett., 35, L01706, doi:10.1029/2007GL032529, 2008.

Thomas, E. R., Hosking, J. S., Tuckwell, R. R., Warren, R. A., and Ludlow, E. C.: Twentieth century increase in snowfall in coastal West Antarctica, Geophys. Res. Lett., 42, 9387–9393, doi:10.1002/2015GL065750, 2015.

Traufetter, F., Oerter, H., Fischer, H., Weller, R., and Miller, H.: Spatio-temporal variability in volcanic sulphate deposition over the past 2 kyr in snow pits and firn cores from Amundsenisen, Antarctica, J. Glaciol., 50, 137–146, doi:10.3189/172756504781830222, 2004.

Turner, J., Colwell, S. R., Marshall, G. J., Lachlan-Cope, T. A., Carleton, A. M., Jones, P. D., Lagun, V., Reid, P. A., and Iagovkina, S.: Antarctic climate change during the last 50 years, Int. J. Climatol., 25, 279–294, doi:10.1002/joc.1130, 2005.

van de Berg, W. J., van den Broeke, M. R., Reijmer, C. H., and van Meijgaard, E.: Reassessment of the Antarctic SMB using calibrated output of a regional atmospheric climate model, J. Geophys. Res., 111, D11104, doi:10.1029/2005JD006495, 2006.

van den Broeke, M., van de Berg, W. J., and van Meijgaard, E.: Snowfall in coastal West Antarctica much greater than previously assumed, Geophys. Res. Lett., 33, L02505, doi:10.1029/2005GL025239, 2006.

Vaughan, D. G., Comiso, J.C., Allison, I., Carrasco, J., Kaser, G., Kwok, R., Mote, P., Murray, T., Paul, F., Ren, J., Rignot, E., Solomina, O., Steffen, K., and Zhang, T.: Observations: Cryosphere, in: Climate Change 2013: The Physical Science Basis. Contribution of Working Group I to the Fifth Assessment Report of the Intergovernmental Panel on Climate Change, edited by: Stocker, T. F., Qin, D., Plattner, G.-K., Tignor, M., Allen, S. K., Boschung, J., Nauels, A., Xia, Y., Bex, V., and Midgley, P. M., Cambridge University Press, Cambridge, United Kingdom and New York, NY, USA, 2013.

Wang, Y., Ding, M., van Wessem, J., Schlosser, E., Altnau, S., van den Broeke, M., Lenaerts, J., Thomas, E., Isaksson, E., Wang, J., and Sun, W.: A comparison of Antarctic Ice Sheet surface mass balance from atmospheric climate models and in situ observations, J. Climate, doi:10.1175/JCLI-D-15-0642.1, early online release, 2016.

Wolff, E. W., Jones, A. E., Bauguitte, S. J.-B., and Salmon, R. A.: The interpretation of spikes and trends in concentration of nitrate in polar ice cores, based on evidence from snow and atmospheric measurements, Atmos. Chem. Phys., 8, 5627–5634, doi:10.5194/acp-8-5627-2008, 2008.

Zhang, M., Li, Z., Ren, J., Xiao, C., Qin, D., Kang, J., and Li, J.: 250 years of accumulation, oxygen isotope and chemical records in a firn core from Princess Elizabeth Land, East Antarctica, J. Geogr. Sci., 16, 23–33, doi:10.1007/s11442-006-0103-5, 2006.